

A unified theory for perfect absorption in ultra-thin absorptive films with reflectors

Jie Luo, Sucheng Li, Bo Hou, Yun Lai*

College of Physics, Optoelectronics and Energy & Collaborative Innovation Center of
Suzhou Nano Science and Technology, Soochow University, Suzhou 215006, China

*laiyun@suda.edu.cn

The maximal absorption rate of ultra-thin films is 50% under the condition that the electric (or magnetic) tangential field is almost constant across the film. However, with certain reflectors, the absorption rate can be greatly increased, to even perfect absorption (100%). In this work, we explicitly derive the general conditions of the ultra-thin absorptive film parameters to achieve perfect absorption with general types of reflectors. We find that the parameters of the film can be classified into three groups, exhibiting: 1) a large permittivity (permeability), 2) a near-zero permeability (permittivity), or 3) a suitable combination of the permittivity and the permeability, respectively. Interestingly, the latter two cases demonstrate extraordinary absorption in ultra-thin films with almost vanishing losses. Our work serves as a guide for designing ultra-thin perfect absorbers with general types of reflectors.

PACS number(s): 41.20.Jb, 42.25.Bs, 78.20.Ci

I. INTRODUCTION

Lossy materials can absorb electromagnetic (EM) wave energy, but if the impedance is mismatched with air, EM waves will be reflected at the surface, leading to inefficiency in energy absorption. To minimize such a reflection and realize perfect absorption (PA), i.e. 100% absorption, several methods have been proposed, including anti-reflection films with a quarter-wavelength thickness [1], micro-structures with gradually varying impedance [2], certain metamaterials [3-10], coherent illumination [11-15], etc.

Ultra-thin absorptive films are an especially interesting class of absorbers. With the thickness much smaller than the wavelength, the phase change of waves inside the film is often negligible, and usually either the electric tangential field or magnetic tangential field is almost constant across the ultra-thin film. Various types of ultra-thin absorbers have been studied in various frequency regimes, including conductive films in microwave and terahertz (THz) regimes [1, 14-16], metal in optical regimes [17-19], organic materials [20], graphene [21], doped semi-conductors [22], epsilon(mu)-near-zero media [23, 24], metamaterial absorber with strong magnetic responses [25], etc. It is known that for such ultra-thin films, the absorption rate is up to 50% [1, 26, 27]. However, such a limit can be broken by introducing symmetrical coherent illumination [15, 16] or specific reflectors. Various types of ultra-thin films with different reflectors have been proposed and demonstrated [1, 16-26], which show that absorption rate >50% is possible. However, a unified theory for ultra-thin absorbers with general reflectors is still lacking.

In this paper, we analytically derive the general solutions of the film parameters for PA for a general class of reflectors characterized by reflected waves with an amplitude η_E ($0 < \eta_E \leq 1$) and a phase shift ϕ_E ($0 \leq \phi_E < 2\pi$). Our work gives a unified theory for designing perfect absorption of ultra-thin films. Specifically, we find the general solutions of the film parameters can be classified into three groups, in which perfect absorption is mainly induced by 1) a large the permittivity (permeability), 2) a near zero permeability (permittivity), or 3) a suitable combination of the permittivity and permeability, for the cases of constant tangential electric (magnetic) field across the film, respectively. Especially, the third case corresponds to perfect absorption at large incident angles, which, to our best knowledge, has not been reported before. Interestingly, although the second and third cases originate in different physical mechanisms, they both demonstrate extraordinary absorption in arbitrarily thin films with almost vanishing loss. Our work serves as a guide to design the ultra-thin film and reflectors for PA.

II. GENERAL SOLUTIONS TO THE PERFECT ABSORPTION

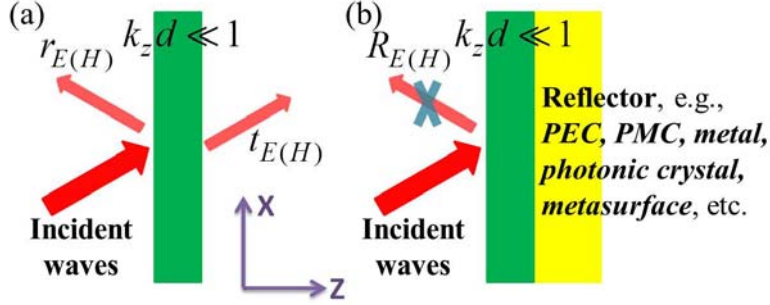


FIG. 1. Schematic graph of the transmission and reflection of EM waves on an ultra-thin absorptive film (a) without and (b) with a reflector attached behind the film.

The system of our investigation is illustrated in Fig. 1(a). In this work, we consider the case in which the film is much thinner compared to the wavelength inside the film, and the phase change across the film is negligible, i.e.

$$k_z^{TE} d = k_0 d \sqrt{\frac{\mu_x}{\mu_z} (\varepsilon_y \mu_z - \sin^2 \theta)} \ll 1 \quad 1(a),$$

$$k_z^{TM} d = k_0 d \sqrt{\frac{\varepsilon_x}{\varepsilon_z} (\mu_y \varepsilon_z - \sin^2 \theta)} \ll 1 \quad 1(b),$$

for transverse electric (TE) polarization (E_y) and transverse magnetic (TM) polarization (H_y), respectively. Here, k_z^{TE} and k_z^{TM} are the z component of wave vectors for TE and TM polarizations, respectively. d , θ , and k_0 are the thickness of the absorption film, the incident angle, and the wave number in free space, respectively.

In such an ultra-thin limit, usually either the electric or magnetic tangential fields are almost constant across the film. This leads to

$$1 + r_{E(H)} \approx t_{E(H)}, \quad (2)$$

where $r_{E(H)}$ and $t_{E(H)}$ are the reflection and transmission coefficients of the film defined on the electric (magnetic) tangential field [28] as illustrated in Fig. 1(a).

If both the electric and magnetic tangential fields are almost constant across the film,

then the transmission is almost unity, and the ultra-thin film does not absorb energy. If only the electric or magnetic tangential field is almost constant across the film, there exists a maximal absorption of 50% which corresponds to $-r_{E(H)} \approx t_{E(H)} \approx 0.5$ [1, 26, 27]. If both the electric and magnetic fields are not constant across the film, then the wavelength inside the film is usually comparable to the film thickness. In this case, there is no 50% absorption limit but there would be Fabry-Perot effects.

In this paper, we will focus on the case in which only the electric or magnetic tangential field is almost constant across the film. For simplicity, we consider the case that only the electric field is almost constant across the film, i.e., $1+r_E \approx t_E$ and $1+r_H \neq t_H$. The case of constant magnetic field can be obtained similarly. By using the transfer matrix method [28] and Eq. (1), we obtain the reflection and transmission coefficients through an ultra-thin film

characterized by relative permittivity (permeability) tensor $\bar{\epsilon}(\bar{\mu}) = \begin{pmatrix} \epsilon(\mu)_x & 0 & 0 \\ 0 & \epsilon(\mu)_y & 0 \\ 0 & 0 & \epsilon(\mu)_z \end{pmatrix}$ as,

$$t_E = \frac{2}{2 - i(f_1^{TE} + f_2^{TE})x^{TE}}, \quad r_E = -\frac{i}{2}t_E(f_1^{TE} - f_2^{TE})x^{TE},$$

$$\text{and } t_H = \frac{2}{2 - i(f_1^{TE} + f_2^{TE})x^{TE}}, \quad r_H = \frac{i}{2}t_H(f_1^{TE} - f_2^{TE})x^{TE} \quad (3a)$$

for TE polarization, and

$$t_E = \frac{2}{2 - i(f_1^{TM} + f_2^{TM})x^{TM}}, \quad r_E = \frac{i}{2}t_E(f_1^{TM} - f_2^{TM})x^{TM},$$

$$\text{and } t_H = \frac{2}{2 - i(f_1^{TM} + f_2^{TM})x^{TM}}, \quad r_H = -\frac{i}{2}t_H(f_1^{TM} - f_2^{TM})x^{TM} \quad (3b)$$

for TM polarization, where $f_1^{TE} = \cos\theta \sqrt{\frac{\mu_x \mu_z}{\epsilon_y \mu_z - \sin^2\theta}}$, $f_2^{TE} = \frac{1}{\cos\theta} \sqrt{\frac{\epsilon_y \mu_z - \sin^2\theta}{\mu_x \mu_z}}$,

$$f_1^{TM} = \cos\theta \sqrt{\frac{\epsilon_x \epsilon_z}{\mu_y \epsilon_z - \sin^2\theta}}, \quad \text{and } f_2^{TM} = \frac{1}{\cos\theta} \sqrt{\frac{\mu_y \epsilon_z - \sin^2\theta}{\epsilon_x \epsilon_z}}, \quad x^{TE} = k_z^{TE} d = k_0 d \sqrt{\frac{\mu_x}{\mu_z} (\epsilon_y \mu_z - \sin^2\theta)},$$

$$\text{and } x^{TM} = k_z^{TM} d = k_0 d \sqrt{\frac{\epsilon_x}{\epsilon_z} (\mu_y \epsilon_z - \sin^2\theta)}.$$

By inserting $1+r_E \approx t_E$ and $1+r_H \neq t_H$ into Eq. (3), we get

$$f_1^{TE} x^{TE} = \cos\theta |\mu_x| k_0 d \approx 0, \quad f_2^{TE} x^{TE} = \frac{1}{\cos\theta} \left| \frac{\varepsilon_y \mu_z - \sin^2\theta}{\mu_z} \right| k_0 d \neq 0 \quad (4a)$$

for TE polarization, and

$$f_2^{TM} x^{TM} = \frac{1}{\cos\theta} \left| \frac{\mu_y \varepsilon_z - \sin^2\theta}{\varepsilon_z} \right| k_0 d \approx 0, \quad f_1^{TM} x^{TM} = \cos\theta |\varepsilon_x| k_0 d \neq 0 \quad (4b)$$

for TM polarization.

Eq. (4) presents the necessary conditions of the film parameters to have almost constant electric field but a variant magnetic field across the film. Under normal incidence, the conditions reduce to $|\mu_x| k_0 d \approx 0$ and $|\varepsilon_y| k_0 d \neq 0$ for TE polarization, and $|\mu_y| k_0 d \approx 0$ and $|\varepsilon_x| k_0 d \neq 0$ for TM polarization. Obviously, such cases satisfy the ultra-thin condition of Eq. (1), which reduces to $k_0 d \sqrt{\mu_x \varepsilon_y} \ll 1$ and $k_0 d \sqrt{\varepsilon_x \mu_y} \ll 1$ in the case of normal incidence.

To break the maximal absorption limit of 50% and achieve PA for such a film, we attach the film with a reflector, as shown in Fig. 1(b). A reflector can be any materials with zero transmission rate, including perfect electric conductor (PEC), perfect magnetic conductor (PMC), lossy metal, photonic crystals within band gaps, reflective high impedance surfaces or meta-surfaces, etc. With reflectors attached, the absorption rate is only associated with reflection rate. Here, we characterize the properties of the reflector by using the amplitude η_E ($0 < \eta_E \leq 1$) and phase shift ϕ_E ($0 \leq \phi_E < 2\pi$) of reflected waves. By using Eq. (2), the total reflection coefficient is obtained as,

$$\begin{aligned} R_E &= (t_E - 1) + t_E \eta_E e^{i\phi_E} t_E + t_E \eta_E e^{i\phi_E} (t_E - 1) \eta_E e^{i\phi_E} t_E + t_E \eta_E e^{i\phi_E} (t_E - 1) \eta_E e^{i\phi_E} (t_E - 1) \eta_E e^{i\phi_E} t_E + \dots \\ &= \frac{(\eta_E^{-1} e^{-i\phi_E} + 2) t_E - \eta_E^{-1} e^{-i\phi_E} - 1}{\eta_E^{-1} e^{-i\phi_E} + 1 - t_E}. \end{aligned} \quad (5)$$

The condition of PA is $R_E = 0$. By letting $R_E = 0$ and considering Eq. (2), we have

$$t_E = \frac{\eta_E^{-1} e^{-i\phi_E} + 1}{\eta_E^{-1} e^{-i\phi_E} + 2} \quad \text{and} \quad r_E = \frac{-1}{\eta_E^{-1} e^{-i\phi_E} + 2}. \quad (6)$$

By inserting Eq. (3) and Eq. (4) into Eq. (6), we analytically obtain the parameter conditions of the ultra-thin film to achieve PA with a reflector of (η_E, ϕ_E) ,

$$\frac{\sin^2 \theta}{\mu_z} - \varepsilon_y + i \frac{2 \cos \theta}{k_0 d (\eta_E^{-1} e^{-i\phi_E} + 1)} = 0 \quad (7a)$$

for TE polarizations, and

$$-\varepsilon_x + i \frac{2}{k_0 d (\eta_E^{-1} e^{-i\phi_E} + 1) \cos \theta} = 0 \quad (7b)$$

for TM polarizations.

Eq. (7) shows many interesting properties for ultra-thin film to achieve PA. For TE polarization, based on Eq. (7), we can classify the solutions into three groups. Case 1).

$\left| \frac{\sin^2 \theta}{\mu_z} \right| \ll |\varepsilon_y| \approx \left| \frac{2 \cos \theta}{k_0 d (\eta_E^{-1} e^{-i\phi_E} + 1)} \right|$. In this case, a large permittivity of $\varepsilon_y = i \frac{2 \cos \theta}{k_0 d (\eta_E^{-1} e^{-i\phi_E} + 1)}$ is

required to achieve PA. Case 2). $|\varepsilon_y| \ll \left| \frac{\sin^2 \theta}{\mu_z} \right| \approx \left| \frac{2 \cos \theta}{k_0 d (\eta_E^{-1} e^{-i\phi_E} + 1)} \right|$. In this case, a small

permeability of $\mu_z = \frac{i}{2} k_0 d (\eta_E^{-1} e^{-i\phi_E} + 1) \sin \theta \tan \theta$ is required to achieve PA. Case 3). The terms

in Eq. 7(a) $\left| \frac{\sin^2 \theta}{\mu_z} \right|$ and $|\varepsilon_y|$ are comparable. In this case, PA can be achieved for a suitable

combination of the permittivity and permeability.

For TM polarization, PA can only be achieved by using a large permittivity

$\varepsilon_x = i \frac{2}{k_0 d (\eta_E^{-1} e^{-i\phi_E} + 1) \cos \theta}$, and is totally independent of the permeability.

Another information that we can retrieve from Eq. (7) is that when $\eta_E^{-1} e^{-i\phi_E} + 1 = 0$, Eq. (7)

can never be satisfied. $\eta_E^{-1} e^{-i\phi_E} + 1 = 0$ leads to $\eta_E = 1$, $\phi_E = \pi$, implying a PEC reflector.

Physically, a PEC reflector forces the tangential electric field to be zero. As a result, the tangential electric field will be zero throughout the film, making PA impossible. As a result, the PEC reflector cannot be applied.

In the following sections, we will discuss in details the three cases for constant tangential electric field across the film, in which PA is due to large permittivity, small permeability, and a suitable combination of the permittivity and permeability, respectively. For the case of constant tangential magnetic field, the previous equations simply need to exchange the permittivity with permeability. As for the case of constant tangential magnetic field, we can

directly refer to the equations above due to the symmetry nature of electric and magnetic fields in the Maxwell's equations.

III. CASE 1: PERFECT ABSORPTION DUE TO LARGE PERMITTIVITY

In case 1 of solutions to Eq. (7), PA for TM polarization is mainly dependent on the value of ε_x . On the other hand, for TE polarization, when $|\mu_z| \gg \left| \frac{k_0 d (\eta_E^{-1} e^{-i\phi_E} + 1)}{2 \cos \theta} \sin^2 \theta \right|$, the condition of PA is reduced to,

$$\varepsilon_y = i \frac{2 \cos \theta}{k_0 d (\eta_E^{-1} e^{-i\phi_E} + 1)} = \frac{2 \cos \theta}{k_0 d} \left(-\frac{\eta_E^{-1} \sin \phi_E}{\eta_E^{-2} + 2\eta_E^{-1} \cos \phi_E + 1} + i \frac{\eta_E^{-1} \cos \phi_E + 1}{\eta_E^{-2} + 2\eta_E^{-1} \cos \phi_E + 1} \right). \quad (8)$$

Under normal incidence with $\theta \rightarrow 0$, $|\mu_z| \gg \left| \frac{k_0 d (\eta_E^{-1} e^{-i\phi_E} + 1)}{2 \cos \theta} \sin^2 \theta \right|$ is always fulfilled.

While under oblique incidence, $|\mu_z| \gg \left| \frac{k_0 d (\eta_E^{-1} e^{-i\phi_E} + 1)}{2 \cos \theta} \sin^2 \theta \right|$ is also satisfied due to ultra-thin thickness $k_0 d \rightarrow 0$, except for the cases of $\theta \rightarrow \pm 90^\circ$ or $|\mu_z| \rightarrow 0$.

A. PMC reflector and coherent illumination

In particular, if the reflector is a PMC with $\eta_E=1$ and $\phi_E=0$, the required relative permittivities will be simplified to,

$$\varepsilon_y = i \frac{\cos \theta}{k_0 d} \quad \text{and} \quad \varepsilon_x = i \frac{1}{k_0 d \cos \theta} \quad (9)$$

for TE and TM polarized waves, respectively. This indicates that pure imaginary permittivities are required for PA with a PMC reflector. Interestingly, metals in low frequency regime naturally exhibit almost pure imaginary permittivity. For a metal with a conductivity σ_0 , the relative permittivity is described as $\varepsilon_r = 1 + i \frac{\sigma(\omega)}{k_0} Z_0 \approx i \frac{\sigma_0}{k_0} Z_0$, where Z_0 is the impedance of free space. Therefore, to obtain the PA, the sheet resistance, R_s , defined as $1/(\sigma_0 d)$, is required to be

$$R_s = 1/(\sigma_0 d) = Z_0 / \cos \theta \quad \text{and} \quad R_s = 1/(\sigma_0 d) = Z_0 \cos \theta \quad (10)$$

for TE and TM polarizations, respectively. Clearly, the required R_s is a function of the incident angle only rather than the operating frequency or film thickness. Such a frequency-independent property indicates that ultra-thin film absorbers without Fabry-Perot effects may be applied to achieve ultra-broadband absorbers, for all frequencies below 100GHz, including radio waves and microwaves. Even in THz regime, some conductive materials can still be exploited, e.g., inconel [16], tungsten [14], graphene [21], to achieve broadband absorption.

To verify the analytical result, we carry out numerical simulations based on the finite element software, COMSOL Multi-physics, as shown in Fig. 2. Figure 2(a) presents the normalized amplitude of total electric field $|\mathbf{E}|/|\mathbf{E}_{in}|$ (blue solid lines) and magnetic field $|\mathbf{H}|/|\mathbf{H}_{in}|$ (red dashed lines) under normal incidence on an ultra-thin conductive film with a PMC reflector. The absorber film on the PMC reflector is characterized by a thickness of $d = \lambda_0 / 100$ and an isotropic relative permittivity of $\epsilon_r = 15.92i$. The unit field amplitude in the free space region indicates there is no reflection and proves the PA. In Fig. 2(a), it is also seen that the electric field is almost constant inside the absorber film, while the amplitude of magnetic field is rapidly decaying in the film. In Fig. 2(b), we plot the absorptance as a function of the incidence angle for such a perfect absorber at normal incidence. Despite that the PA condition is broken for oblique incidence, it is seen that high absorptance rate >0.9 is observed in a wide angle range. By applying the transfer matrix method, we find that both the absorptance for TE and TM polarized waves can be written as

$$A = 1 - \tan^4(\theta/2), \quad (11)$$

which is confirmed by numerical simulation as shown in Fig. 2(b).

Although we have shown above that ultra-thin film with suitable resistance and a PMC reflector can realize PA. However, the realization of PMC reflector itself is another important issue. Recently, high impedance surfaces or meta-surfaces have also been extensively investigated and they can work as effective PMCs [29-32]. These structures are deep

sub-wavelength, and support engineering of the amplitude η_E and phase change ϕ_E of reflected waves. In most cases, although ϕ_E can be tuned to be zero, but η_E would be smaller than unity. In Figs. 2(c) and 2(d) we plot the required sheet resistance R_s and the ratio $|\text{Re}(\epsilon_r)/\text{Im}(\epsilon_r)|$ as the function of η_E and ϕ_E , respectively. It is seen that the influence of phase shift ϕ_E on R_s is weak while decreased η_E leads to increased R_s . However, the real part $\text{Re}(\epsilon_r)$ increases rapidly with increased ϕ_E , but is insensitive to changes in η_E .

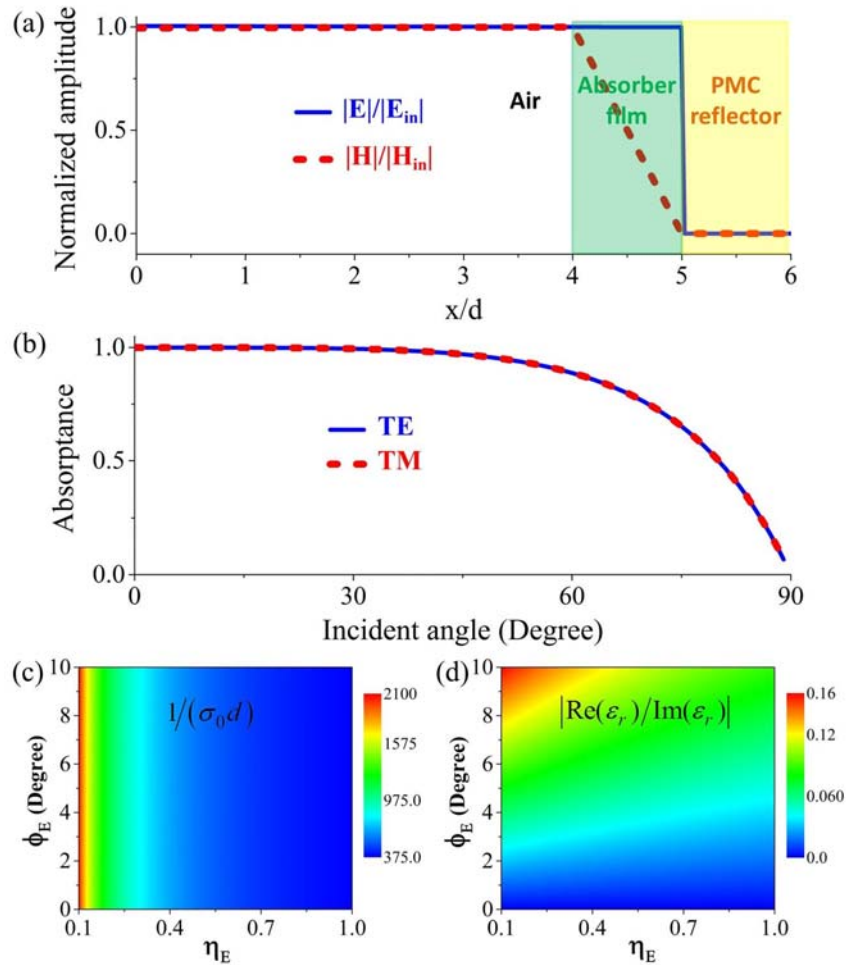


FIG. 2. (a) The normalized amplitude electric field $|\mathbf{E}|/|\mathbf{E}_{in}|$ (blue solid lines) and magnetic field $|\mathbf{H}|/|\mathbf{H}_{in}|$ (red dashed lines) in the case of PA on an ultra-thin film characterized by $\epsilon_r = 15.92i$, $\mu_r = 1$ and $d = \lambda_0/100$ with a PMC reflector under normal incidence. (b)

Absorptance as a function of the incident angle for both TE (black solid lines) and TM (red dashed lines) polarizations. (c) The required sheet resistance $1/(\sigma_0 d)$ for the PA and (d) the ratio $|\text{Re}(\epsilon_r)/\text{Im}(\epsilon_r)|$ as the function of the η_E and ϕ_E under normal incidence.

Besides high impedance surfaces and meta-surfaces, other methods for mimicking PMC include PEC coated with a high-index dielectric layer with optical thickness $\lambda_0/4$ [1, 16, 21, 26, 33] or an anisotropic layer through transformation optics [34], dielectric Bragg mirror with a spacer layer [24], or epsilon-near-zero media with dielectric defects [35], etc. However, these methods require a finite thickness of the wavelength order.

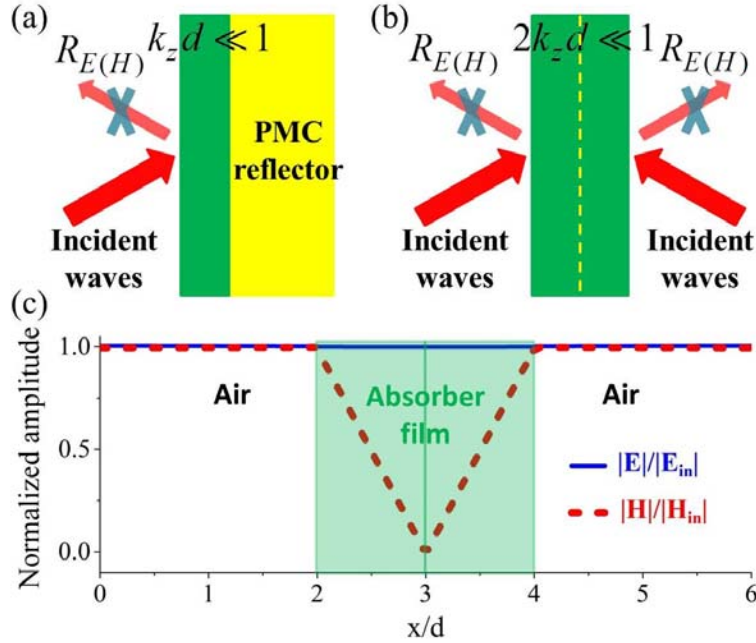


FIG. 3. Schematic graphs of (a) an ultra-thin absorber film with a PMC reflector attached, (b) an equivalent double-layered absorber film with waves symmetrically incident from both sides. (c) The normalized amplitude electric field $|E|/|E_{in}|$ (blue solid lines) and magnetic field $|H|/|H_{in}|$ (red dashed lines) under normal incidence for symmetrical illumination. The absorber film is characterized by $\epsilon_r = 15.92i$, $\mu_r = 1$ and $d = \lambda_0/50$.

The bandwidth of PA lies in the bandwidth of the PMC reflector. Actually, a PMC reflector is equivalent to a special mirror. The absorber film with a PMC reflector is equivalent to a double-layered absorber film with symmetrical coherent illumination, as illustrated in Figs. 3(a) and 3(b). According to Eq. (3), the reflection and transmission coefficients of the double-layered film are $r_E = -0.5$ and $t_E = 0.5$. Thus, the total reflection coefficient $R_E = r_E + t_E = 0$. Figure 3(c) shows the normalized amplitude distribution in the double-layered absorber film with a total thickness of $d = \lambda_0/50$. The relative permittivity and relative permeability are chosen as $\epsilon_r = 15.92i$ and $\mu_r = 1$, respectively, which are the same as those in Fig. 2(a). The incoming waves normally incident from both side in a symmetrical manner. It is seen from Fig. 3(c) that the normalized amplitude of electric field in both air and absorber regions is nearly unity, indicating almost PA. However, the magnetic field amplitude exhibits a dip at the center. In such a way, the bandwidth of PMC reflector can be avoided and ultra-broadband absorption is indeed possible. Po et al. have theoretically shown that a 17nm tungsten film can absorb most of the incident waves in the frequency range from 200THz to 800THz [14]. Recently, we have experimentally demonstrated a good performance of PA by using ultra-thin conductive films in the microwave regime [15]. It is verified that the PA is indeed independent of frequency for a suitable conductivity.

B. Other phase-controllable and absorptive reflectors

In most practical cases, the reflector has a reflection amplitude less than unity and a reflection shift ϕ_E substantially different from 0 and π . In high frequency regime, such as infrared and optical frequencies, the PMC reflectors and absorber films with large pure imaginary part are difficult to achieve. Reflectors such as dielectric Bragg mirror [20], meta-surfaces [3], metal [17, 19] and sapphire [18, 22] which can induce a reflection shift ϕ_E substantially different from 0 and π and result in a complex value of $\eta_E^{-1} e^{-i\phi_E}$, have also been investigated. As a consequence, the required permittivity is also a complex number as described by Eqs.

(7b) and (8), instead of a pure imaginary number as in the case of PMC reflectors. Particularly, under normal incidence, the required permittivities turn out to be,

$$\varepsilon_x = \varepsilon_y = \frac{2}{k_0 d} \left(-\frac{\eta_E^{-1} \sin \phi_E}{\eta_E^{-2} + 2\eta_E^{-1} \cos \phi_E + 1} + i \frac{\eta_E^{-1} \cos \phi_E + 1}{\eta_E^{-2} + 2\eta_E^{-1} \cos \phi_E + 1} \right) \quad (12)$$

Here, we demonstrate a specific example which was described in Ref. [17]. Suppose that the working wavelength is $\lambda_0 = 532 \text{ nm}$ and the reflector is selected as gold characterized by a refractive index of $n_{\text{Gold}} = 0.44 + 2.24i$. The thickness of the absorber film is fixed as $d = 10 \text{ nm}$. Through Eq. (12), we can easily calculate the required refractive index of the absorber film for PA as $n = \sqrt{\varepsilon_x} = \sqrt{\varepsilon_y} = 4.39 + 0.54i$, which is quite near the value $n = 4.3 + 0.71i$ found by Kats et al [17] through numerically searching. Our unified theory can provide a simple way to obtain required parameters of ultra-thin film and reflector for PA.

IV. CASE 2: PERFECT ABSORPTION DUE TO SMALL PERMEABILITY

Here, we consider a situation with $|\varepsilon_y| \ll \left| \frac{\sin^2 \theta}{\mu_z} \right| \approx \left| \frac{2 \cos \theta}{k_0 d (\eta_E^{-1} e^{-i\phi_E} + 1)} \right|$ (see Eq. (7)) for the case of continuous tangential electric field. In this case, the condition of the PA for TE polarized waves is

$$\mu_z = \frac{i}{2} k_0 d (\eta_E^{-1} e^{-i\phi_E} + 1) \sin \theta \tan \theta, \quad (13)$$

and is less dependent on the permittivity of the absorber film. If the reflector is nearly a PMC, we have,

$$\text{Re}(\mu_z) \ll \text{Im}(\mu_z) \rightarrow 0 \quad \text{and} \quad \frac{d}{\lambda_0} = \frac{\text{Im}(\mu_z)}{2\pi \sin \theta \tan \theta}. \quad (14)$$

On the other hand, if the tangential magnetic field is almost constant inside the absorber film, we get $\text{Re}(\varepsilon_z) \ll \text{Im}(\varepsilon_z) \rightarrow 0$ and $\frac{d}{\lambda_0} = \frac{\text{Im}(\varepsilon_z)}{2\pi \sin \theta \tan \theta}$ for TM polarizations, which have been theoretically demonstrated by Feng et al. [24].

Although such PA is only achievable for oblique incidence [23, 24], and generally works for narrow band due to intrinsically dispersive zero-index materials [36-42], one interesting advantage of such PA is that there exists a linear relationship between the thickness and the

loss, which means that the thickness of the absorber can be pushed to zero by reducing the material loss to zero. As a result, an arbitrarily thin perfect absorber with near-zero value parameters is possible [23, 24], which is different from common understanding that thinner absorber film needs a larger absorption part to maintain the same absorption.

To clarify the physical origin of the extraordinary absorption, we numerically study an ultra-thin film characterized by $\mu_z = 0.01814i$, $\mu_x = \varepsilon = 1$ and $d = \lambda_0/100$ with a PMC reflector attached. TE polarized waves are incident from air under an incident angle of $\theta = 30\text{deg}$. The normalized amplitude distribution in Fig. 4 confirms the homogeneous electric fields E_y (blue solid lines) and the decaying x-component of magnetic field H_x (red dashed lines) inside the film. It is also seen that the z-component magnetic field H_z (purple dashed lines) is enhanced by about 55 times in the absorber film, which is required by the continuity of B_z at the interface. H_z increases rapidly as the decrease of the thickness of the absorber film, leading to the extraordinary absorption in the ultra-thin film.

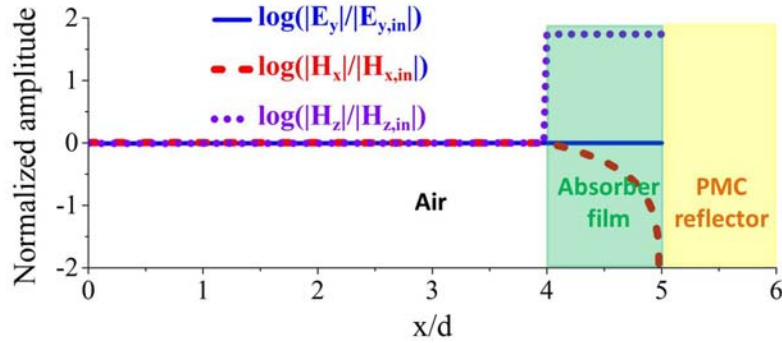


FIG. 4. The normalized amplitude electric field $\log(|E_y|/|E_{y,in}|)$ (blue solid lines), x-component of magnetic field $\log(|H_x|/|H_{x,in}|)$ (red dashed lines) and z-component of magnetic field $\log(|H_z|/|H_{z,in}|)$ (purple dotted lines) for EM waves of TE polarization incident on an absorber film characterized by $\mu_z = 0.01814i$, $\mu_x = \varepsilon = 1$ and $d = \lambda_0/100$ with a PMC reflector under the incidence angle of $\theta = 30\text{deg}$.

V. CASE 3: PERFECT ABSORPTION DUE TO A SUITABLE COMBINATION OF PERMITTIVITY AND PERMEABILITY

Now we consider the case that PA is induced by a suitable combination of the permittivity and permeability of the absorber film when $\left| \frac{\sin^2 \theta}{\mu_z} \right|$ and $|\varepsilon_y|$ are comparable, i.e.

$$\left| \frac{2 \cos \theta}{k_0 d (\eta_E^{-1} e^{-i\phi_E} + 1)} \right| \ll \left| \frac{\sin^2 \theta}{\mu_z} \right| \approx |\varepsilon_y| \quad \text{or} \quad |\varepsilon_y| \sim \left| \frac{\sin^2 \theta}{\mu_z} \right| \sim \left| \frac{2 \cos \theta}{k_0 d (\eta_E^{-1} e^{-i\phi_E} + 1)} \right|. \quad \text{For a film with a fixed } k_0 d$$

and under oblique incidence, when $\theta \rightarrow \pm 90 \text{ deg}$ or $\eta_E \rightarrow 0$, we have $\left| \frac{2 \cos \theta}{k_0 d (\eta_E^{-1} e^{-i\phi_E} + 1)} \right| \rightarrow 0$

and the PA would depend on a suitable choice of μ_z and ε_y . $\eta_E \rightarrow 0$ indicates that the reflector alone can absorb a lot of the incident waves and there is less need for the film.

However, when $\theta \rightarrow \pm 90 \text{ deg}$, we find the condition of PA turns into $\frac{1}{\mu_z} - \varepsilon_y \approx 0$. That is, as

the increase of the incident angle, the real part of $\varepsilon_y \mu_z$ tends to be unity, while its imaginary part tends to zero. This indicates that a vanishing loss is capable of achieving PA for the case of very large incident angle, similar to the extraordinary absorption in the near zero permeability film in the case 2. However, the physical origin is totally different. The extraordinary high absorption in the zero-index media is caused by the greatly enhanced fields in the longitudinal direction. While here, it is seen that when $\theta \rightarrow \pm 90 \text{ deg}$, we have

$\sqrt{\mu_z \varepsilon_y} \approx 1$, which means that the absorber film has a refractive index close to that of air, as illustrated by Fig. 5(a). So the waves propagate almost along the x direction in phase with the waves in air, and therefore have an extremely long absorption distance. Eventually, the waves are gradually absorbed with a tiny loss.

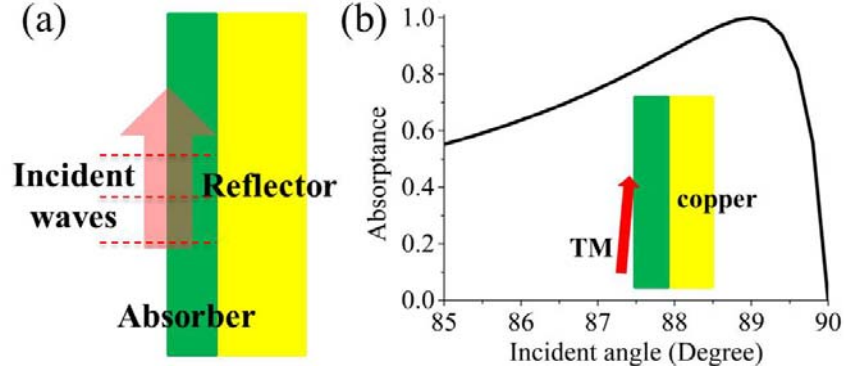


FIG. 5. (a) Schematic graph of PA when waves are incident on the ultra-thin absorptive film with extremely large angles, i.e. $\theta \rightarrow \pm 90$ deg. The waves in the ultra-thin film and air are in phase. (b) The absorbance as the function of the incident angle for an absorber film with $\varepsilon = 0.9278 + 0.2565i$, $\mu = 1$ and $d = \lambda_0/100$. The reflector is chosen as copper with DC conductivity being $\sigma_0 = 6.5 \times 10^7 \Omega^{-1} m^{-1}$.

In most practical cases, the situation $|\varepsilon_y| \sim \left| \frac{\sin^2 \theta}{\mu_z} \right| \sim \left| \frac{2 \cos \theta}{k_0 d (\eta_E^{-1} e^{-i\phi_E} + 1)} \right|$ is satisfied under oblique incidence. Here we take an example of constant tangential magnetic field, which requires $\left| \frac{\sin^2 \theta}{\varepsilon_z} \right| \sim |\mu_y| \sim \left| \frac{2 \cos \theta}{k_0 d (\eta_H^{-1} e^{-i\phi_H} + 1)} \right|$ for TM polarized waves. We exploit practical copper as the reflector, whose DC conductivity is about $\sigma_0 = 6.5 \times 10^7 \Omega^{-1} m^{-1}$, the required relative permeability of the absorber film with $\mu = 1$ and $d = \lambda_0/100$ calculated from Eq. (7) is $\varepsilon = 0.9278 + 0.2565i$ under an incident angle of $\theta = 89$ deg. Moreover, we plot the absorbance with respect to the incident angle in Fig. 5(b), showing that the absorption is indeed sensitive to the variation of incident angle.

VI. CONCLUSION

In conclusion, we have explicitly derived the general solutions to the PA for an ultra-thin absorptive film with a general reflector. The cases of constant tangential electric field are

investigated in details. We find the solutions for TE polarization can be classified to three groups in which PA is induced by large permittivity, small permeability or a suitable combination of permittivity and permeability. The solutions for TM polarization can only be induced by large permittivity. To give a clear picture of this theory, we have prepared a figure describe the outline in the Supplementary Material [43]. Based on our theory, we have not only physically explained results in previous literature, but also found new mechanisms to achieve PA. Especially, we find that ultra-thin conductive films with a PMC reflector can achieve frequency-independent PA, which has the same principle as the PA achieved under symmetrical coherent illumination. We also find a new type of PA mechanism for large incident angle (case 3), which might be useful to achieve perfect absorption in waveguide structures. Although the cases in this paper were demonstrated for constant tangential electric field, similar analyses would easily be applied to the cases of constant tangential magnetic field due to the symmetry nature of electric and magnetic fields in the Maxwell's equations.

Finally, we note that our current theory has considered the ultra-thin film and the reflectors to be homogeneous materials or effective media. The cases that there are inhomogeneities in the film or reflectors such as patterns, cavities, etc., the effective medium approximation must also take the influence of surface waves into account, which we will discuss elsewhere in detail.

ACKNOWLEDGEMENTS

This work is supported by the State Key Program for Basic Research of China (No. 2012CB921501), National Natural Science Foundation of China (No. 11104196, No.11104198, No. 11374224), Natural Science Foundation of Jiangsu Province (No. BK2011277), Program for New Century Excellent Talents in University (NCET), and a Project Funded by the Priority Academic Program Development of Jiangsu Higher Education Institutions (PAPD).

REFERENCES

- [1] B. A. Munk, *Frequency Selective Surfaces, Theory and Design* (Wiley, New York, 2000).
- [2] E. F. Knott, J. F. Schaeffer, and M. T. Tuley, *Radar Cross Section* (Artech House, 1993).

- [3] N. Engheta, "Thin absorbing screens using metamaterial surfaces," *IEEE Ant. Propagat. Soc. Internat. Symp.* **2**, 392 (2002).
- [4] N. I. Landy, S. Sajuyigbe, J. J. Mock, D. R. Smith, and W. J. Padilla, "Perfect metamaterial absorber," *Phys. Rev. Lett.* **100**, 207402 (2008).
- [5] H. Tao, C. M. Bingham, A. C. Strikwerda, D. Pilon, D. Shrekenhamer, N. I. Landy, K. Fan, X. Zhang, W. J. Padilla, and R. D. Averitt, "Highly flexible wide angle of incidence terahertz metamaterial absorber: Design, fabrication, and characterization," *Phys. Rev. B* **78**, 241103 (2008).
- [6] H. Tao, N. I. Landy, C. M. Bingham, X. Zhang, R. D. Averitt, and W. J. Padilla, "A metamaterial absorber for the terahertz regime: Design, fabrication and characterization," *Opt. Express* **16**, 7181 (2008).
- [7] X. Liu, T. Starr, A. F. Starr, and W. J. Padilla, "Infrared spatial and frequency selective metamaterial with near-unity absorbance," *Phys. Rev. Lett.* **104**, 207403 (2010).
- [8] H.-T. Chen, J. Zhou, J. F. O'Hara, F. Chen, A. K. Azad, and A. J. Taylor, "Antireflection coating using metamaterials and identification of its mechanism," *Phys. Rev. Lett.* **105**, 073901 (2010).
- [9] D. Ye, Z. Wang, K. Xu, H. Li, J. Huangfu, Z. Wang, and L. Ran, "Ultrawideband dispersion control of a metamaterial surface for perfectly-matched-layer-like absorption," *Phys. Rev. Lett.* **111**, 187402 (2013).
- [10] L. Huang and H.-T. Chen, "A Brief review on terahertz metamaterial perfect absorbers," *Terahertz Sci. Technol.* **6**, 26 (2013).
- [11] Y. D. Chong, L. Ge, H. Cao, and A. D. Stone, "Coherent perfect absorbers: time-reversed lasers," *Phys. Rev. Lett.* **105**, 053901 (2010).
- [12] W. Wan, Y. Chong, L. Ge, H. Noh, A. D. Stone, and H. Cao, "Time-reversed lasing and interferometric control of absorption," *Science* **331**, 889 (2011).
- [13] H. Noh, Y. Chong, A. D. Stone, and H. Cao, "Perfect coupling of light to surface plasmons by coherent absorption," *Phys. Rev. Lett.* **108**, 186805 (2012).
- [14] M. Pu, Q. Feng, M. Wang, C. Hu, C. Huang, X. Ma, Z. Zhao, C. Wang, and X. Luo, "Ultrathin broadband nearly perfect absorber with symmetrical coherent illumination," *Opt. Express* **20**, 2246 (2012).
- [15] S. Li, J. Luo, S. Anwar, S. Li, W. Lu, Z. H. Hang, Y. Lai, B. Hou, M. Shen, and C.-H. Wang, Submitted.
- [16] A. J. Gatesman, A. Danylov, T. M. Goyette, J. C. Dickinson, R. H. Giles, W. Goodhue, J. Waldman, W. Nixon, and W. Hoen, "Terahertz behavior of optical components and common materials," *Proc. SPIE* **6212**, 62120E (2006).
- [17] M. A. Kats, R. Blanchard, P. Genevet, and F. Capasso, "Nanometre optical coatings based on strong interference effects in highly absorbing media," *Nat. Mater.* **12**, 20 (2013).
- [18] M. A. Kats, D. Sharma, J. Lin, P. Genevet, R. Blanchard, Z. Yang, M. M. Qazilbash, D. N. Basov, S. Ramanathan, and F. Capasso, "Ultra-thin perfect absorber employing a tunable phase change material," *Appl. Phys. Lett.* **101**, 221101 (2012).
- [19] M. A. Kats, S. J. Byrnes, R. Blanchard, M. Kolle, P. Genevet, J. Aizenberg, and F. Capasso, "Enhancement of absorption and color contrast in ultra-thin highly absorbing optical coatings," *Appl. Phys. Lett.* **103**, 101104 (2013).
- [20] J. R. Tischler, M. S. Bradley, and V. Bulović, "Critically coupled resonators in vertical geometry using a planar mirror and a 5 nm thick absorbing film," *Opt. Lett.* **31**, 2045 (2006).
- [21] J. M. Woo, M.-S. Kim, H. W. Kim, and J.-H. Jang, "Graphene based salisbury screen for terahertz absorber," *Appl. Phys. Lett.* **104**, 081106 (2014).
- [22] J. W. Cleary, R. Soref, and J. R. Hendrickson, "Long-wave infrared tunable thin-film perfect absorber utilizing highly doped silicon-on-sapphire," *Opt. Express* **21**, 19363 (2013).
- [23] Y. Jin, S. Xiao, N. A. Mortensen, and S. He, "Arbitrarily thin metamaterial structure for perfect absorption

- and giant magnification " *Opt. Express* **19**, 11114 (2011).
- [24] S. Feng and K. Halterman, "Coherent perfect absorption in epsilon-near-zero metamaterials," *Phys. Rev. B* **86**, 165103 (2012).
- [25] S. Zhong and S. He, "Ultrathin and lightweight microwave absorbers made of mu-near-zero metamaterials," *Sci. Rep.* **3**, 2083 (2013).
- [26] C. Hilsum, "Infrared absorption of thin metal films," *J. Opt. Soc. Am.* **44**, 188 (1954).
- [27] S. Li, S. Anwar, W. Lu, Z. H. Hang, B. Hou, M. Shen, and C.-H. Wang, "Microwave absorptions of ultrathin conductive films and designs of frequency-independent ultrathin absorbers," *AIP Adv.* **4**, 017130 (2014).
- [28] D. W. Berreman, "Optics in stratified and anisotropic media: 4 X 4-matrix formulation," *J. Opt. Soc. Am.* **62**, 502 (1972).
- [29] K.-P. Ma, K. Hirose, F.-R. Yang, Y. Qian, and T. Itoh, "Realisation of magnetic conducting surface using novel photonic bandgap structure," *Electron. Lett.* **34**, 2041 (1998).
- [30] F.-R. Yang, K.-P. Ma, Y. Qian, and T. Itoh, "A uniplanar compact photonic-bandgap (UC-PBG) structure and its applications for microwave circuit," *IEEE Trans. Microwave Theory Tech.* **47**, 1509 (1999).
- [31] F.-R. Yang, K.-P. Ma, Y. Qian, and T. Itoh, "A novel TEM waveguide using uniplanar compact photonic-bandgap (UC-PBG) structure," *IEEE Trans. Microwave Theory Tech.* **47**, 2092 (1999).
- [32] D. Sievenpiper, L. Zhang, R. F. J. Broas, N. G. Alexopolous, and E. Yablonovitch, "High-impedance electromagnetic surfaces with a forbidden frequency band," *IEEE Trans. Microwave Theory Tech.* **47**, 2059 (1999).
- [33] P.-S. Kildal, A. A. Kishk, and A. Tengs, "Reduction of forward scattering from cylindrical objects using hard surfaces," *IEEE Trans. Antenna Propagat.* **44**, 1509 (1996).
- [34] F. Liu, Z. Liang, and J. Li, "Manipulating polarization and impedance signature: a reciprocal field transformation approach," *Phys. Rev. Lett.* **111**, 033901 (2013).
- [35] T. Wang, J. Luo, L. Gao, P. Xu, and Y. Lai, "Equivalent perfect magnetic conductor based on epsilon-near-zero media," *Appl. Phys. Lett.* accepted.
- [36] S. Enoch, G. Tayeb, P. Sabouroux, N. Guerin, and P. Vincent, "A metamaterial for directive emission," *Phys. Rev. Lett.* **89**, 213902 (2002).
- [37] M. Silveirinha and N. Engheta, "Tunneling of electromagnetic energy through subwavelength channels and bends using ϵ -near-zero materials," *Phys. Rev. Lett.* **97**, 157403 (2006).
- [38] X. Huang, Y. Lai, Z. H. Hang, H. Zheng, and C. T. Chan, "Dirac cones induced by accidental degeneracy in photonic crystals and zero-refractive-index materials," *Nat. Mater.* **10**, 582 (2012).
- [39] N. Engheta, "Pursuing near-zero response," *Science* **340**, 286 (2013).
- [40] R. Maas, J. Parsons, N. Engheta, and A. Polman, "Experimental realization of an epsilon-near-zero metamaterial at visible wavelengths," *Nat. Photon.* **7**, 907 (2013).
- [41] P. Moitra, Y. Yang, Z. Anderson, I. I. Kravchenko, D. P. Briggs, and J. Valentine, "Realization of an all-dielectric zero-index optical metamaterial," *Nat. Photon.* **7**, 791 (2013).
- [42] J. Luo, W. Lu, Z. Hang, H. Chen, B. Hou, Y. Lai, and C. T. Chan, "Arbitrary control of electromagnetic flux in inhomogeneous anisotropic media with near zero index," *Phys. Rev. Lett.* **112**, 073903 (2014).
- [43] See supplemental material for the outlines of this theory.